The QS- and IS-parameters obtained are given in Table 1. The parameter values depend on such factors as the local symmetry, the type of ligand, and so on; we note that the QS is zero for bulk metal, in view of the cubic symmetry. Furthermore, the IS values are given with respect to that for ^{197}Au in bulk Pt metal (-1.22 mm s^{-1}), earlier determined for Au foil relative to a ^{197}Au : Pt (bulk) source[13].

The most striking feature in Table 1 is that the IS of the inner-core sites in $^{197}AuPt^{+}_{308}$ equals, within the experimental error of ± 0.05 mm s^{-1}, that found for ^{197}Au in bulk Pt. As the interatomic distance for this cluster is also equal to the Pt bulk value, this warrants the conclusion that the 147 atoms of the inner core behave as a minute piece of bulk Pt (the IS depends sensitively on interatomic distance). For the 13-atom inner core of the Au_{55} clusters, we have found (in earlier studies) small but significant deviation of the IS from the bulk value. The interatomic distance in Au_{55} is also ~3% smaller than in the bulk[6,7].

The implication seems to be that for $Pt_{309}Phen^{*}_{36}O_{30\pm10}$ the effects of charge transfer between ligands and metal atoms, as seen by Mössbauer spectroscopy, are restricted to the first layer of surface atoms. This is perhaps not unexpected as far as the Au 5*d* electron density is concerned, as the *d*-orbitals are known to have strongly localized character. The IS value, however, probes mainly the density of the more itinerant 6*s* electrons, and it is therefore interesting in itself that for the inner atoms no measurable effect of the surface-ligation is seen. We note that the 'metallic' behaviour for the inner-core atoms in $Pt_{309}Phen^{*}_{36}O_{30\pm10}$ has also been inferred from the low-temperature specific heat[9], as well as from ^{195}Pt-NMR measurements[8]. A discussion of these results falls outside the scope of this Letter.

Lastly we comment on the parameter values found for the other sites. The values of IS and QS for atoms at sites coordinated by Phen* and O_2 are in a region common for Au surface atoms in clusters[7], and for various linearly coordinated, nominally Au(I) compounds, as might be expected. It is surprising that the unligated surface sites exhibit a QS value of zero, with an IS corresponding to nominally Au(V) compounds. On the other hand, similar values have been found for (central) Au atoms in small Au clusters, such as Au_8, Au_9 and Au_{11} (see, for example, ref. 6 and references therein). None the less, we have at present no explanation for this result.

Further refinement and examination of alternative models for the location of O_2 molecules (and thus of part of the bare surface sites) is in progress. But the IS obtained for the core sites will not be substantially influenced by alternative choices for the different surface sites, nor by improvement of statistics and by further refinement, and our conclusion that the core sites experience an *s*-electron density comparable to that observed for an Au atom in bulk Pt metal should not be sensitive to these refinements. □

Received 12 August; accepted 13 December 1993.

1. Moskovits, M. (ed.) *Metal Clusters* (Wiley, New York, 1986).
2. De Jongh, L. J. *et al.* in *Physics and Chemistry of Finite Systems: From Clusters to Crystals* Vol. 2 (eds Jena, P. *et al.*) 839–851 (Kluwer, Dordrecht, 1992).
3. Schmid, G. *Chem. Rev.* **92,** 1709–1727 (1991).
4. Schmid, G., Morun, B. & Malm, J. O. *Angeur. Chem. int. Edn engl.* **28,** 778–780 (1989).
5. Smit, H. H. A., Nugteren, P. R., Thiel, R. C. & de Jongh, L. J. *Physica* B**153,** 33–52 (1988).
6. Thiel, R. C., Benfield, R. E., Zanoni, R., Smit, H. H. A. & Dirken, M. W. *Struct. Bonding* **81,** 1–39 (1993).
7. Mulder, F. M., van der Zeeuw, E. A., Thiel, R. C. & Schmid, G. *Solid St. Commun.* **85,** 93–97 (1993).
8. van der Putten, D., Brom, H. B., de Jongh, L. J. & Schmid, G. in *Physics and Chemistry of Finite Systems From Clusters to Crystals* Vol. 2 (eds Jena, P. *et al.*) 1007 (Kluwer, Dordrecht, 1992); *Z. Phys.* D**26,** S21–24 (1993).
9. Baak, J., Brom, H. B., de Jongh, L. J. & Schmid, G. *Z. Phys.* D**26,** S30–33 (1993).
10. Simopoulos, A. & Vogl, S. *Phys. Status Solidi* **59,** 505–527 (1973).
11. van Staveren, M. P. J., Brom, H. B. & de Jongh, L. J. *Phys. Rep.* **208,** 1–96 (1991).
12. Viegers, M. P. A. & Trooster, J. M. *Phys. Rev.* B**15,** 72–83 (1977).
13. Shenoy, G. K. & Wagner, F. E. *Mössbauer Isomer Shifts* 906, (North Holland, Amsterdam, 1978).

ACKNOWLEDGEMENTS. We thank P.C.M. Gubbins and the Interfaculty Reaction Institute of the Delft University of Technology for providing the neutron irradiation facilities. This work was supported by the Nederlandse Organisatie voor Wetenschappelijk Onderzoek and the European Union.

Gas-phase self-assembly of endohedral metallofullerenes

David E. Clemmer, Konstantin B. Shelimov & Martin F. Jarrold

Department of Chemistry, Northwestern University, 2145 Sheridan Road, Evanston, Illinois 60208, USA

METALLOFULLERENES[1,2] **consist of metal atoms trapped inside closed fullerene cages. Virtually nothing is known about the mechanism of metallofullerene synthesis, although the possibility of a condensed-phase mechanism has been suggested in recent studies[3,4]. Here we show that laser vaporization of a La_2O_3/graphite rod produces a number of LaC_{60}^{+} isomers, including the endohedral metallofullerene and a variety of different isomers in which lanthanum seems to be bound to polycyclic polyyne rings. When heated, nearly all of the different ring isomers convert spontaneously into metallofullerenes, trapping the metal atom inside the fullerene cage with remarkably high efficiency (>98%). We suggest that in the first step of this annealing process the lanthanum atom acts as a nucleation centre and the carbon rings arrange themselves around the lanthanum atom before converting into a fullerene cage.**

Recent studies have shown that fullerenes can be synthesized by annealing polycyclic polyyne rings[5–7]. The work described here was undertaken to determine whether a similar mechanism could result in the formation of metallofullerenes. The experimental approach has been described previously[6,8]. LaC_{60}^{+} ions were generated by laser vaporization of a La_2O_3/graphite composite rod[1], and selected with a quadrupole mass spectrometer. Pulses (50 μs) of LaC_{60}^{+} ions were injected (at various kinetic energies) into a drift tube containing ~5 torr of He. The ions travel across the drift tube under the influence of a weak electric field, and the drift time depends on the geometry of the cluster[9]. Clusters with compact geometries have shorter drift times than clusters with less compact geometries.

Figure 1 shows the drift-time distributions recorded for C_{60}^{+} and LaC_{60}^{+} using low injection energies. These distributions essentially reflect the isomer populations generated by the source. The distribution for C_{60}^{+} has been discussed in detail previously[6]. The narrow peak at ~800 μs is due to the fullerene, and the broad distribution centred at ~1,600 μs has been assigned to a variety of polycyclic polyyne ring isomers[9], like the bicyclic ring shown in Fig. 1. The drift-time distribution for LaC_{60}^{+} has a narrow peak at ~800 μs that we assign to the endohedral metallofullerene (see below) and a broad distribution of non-fullerene isomers extending out to drift times of ~2,000 μs. The distribution of non-fullerene isomers for LaC_{60}^{+} is broader than observed for C_{60}^{+}. The LaC_{60}^{+} isomers with drift times of ~1,300–2,000 μs are probably due to La^{+} attached to roughly planar polycyclic polyyne ring isomers similar to those observed for the pure carbon cluster. The LaC_{60}^{+} isomers with drift times of ~800–1,300 μs are less compact than the metallofullerene, but more compact than the planar polycyclic rings. These are probably three-dimensional complexes of La^{+} with polyyne rings, although the precise nature of the bonding is not known. The relative abundance of the non-fullerene LaC_{60}^{+} isomers in Fig. 1 is ~50%. The relative abundances of the different non-fullerene isomers were sensitive to the source conditions. The results shown in Fig. 1 are an average of three typical data sets.

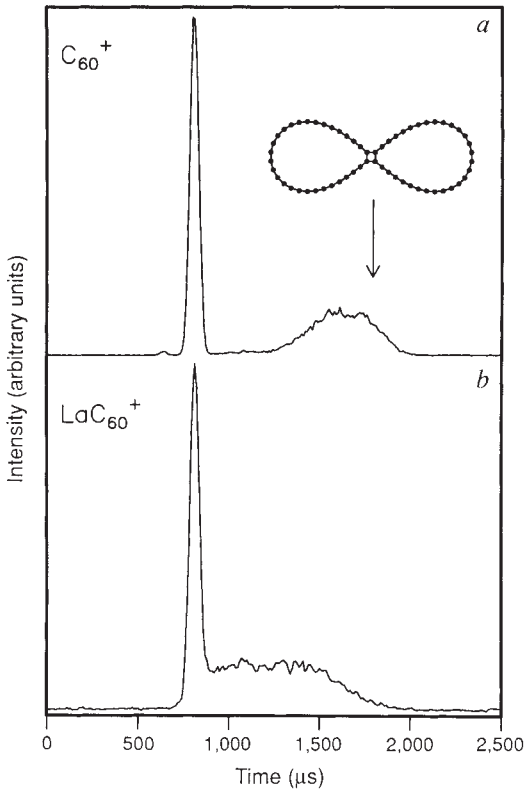

FIG. 1 Drift-time distributions recorded for *a* C_{60}^+ with an injection energy of 100 eV, and *b*, LaC_{60}^+ with an injection energy of 50 eV. The drift tube is 7.62 cm long and the drift field was 13.12 V cm^{-1}. The drift-time distributions have been scaled to a helium buffer gas pressure of 5.00 torr. With the injection energies employed here the isomer populations essentially reflect those generated by the source. The mass spectrum generated by laser vaporization of the La_2O_3/graphite rod is dominated by peaks due to LaC_n^+ and C_n^+. However, measurements of the isotope distributions show that the peaks were not entirely pure LaC_{60}^+. Studies were performed as a function of isotopic composition and we are confident that the data presented here result from ions which are predominantly (>95%) LaC_{60}^+.

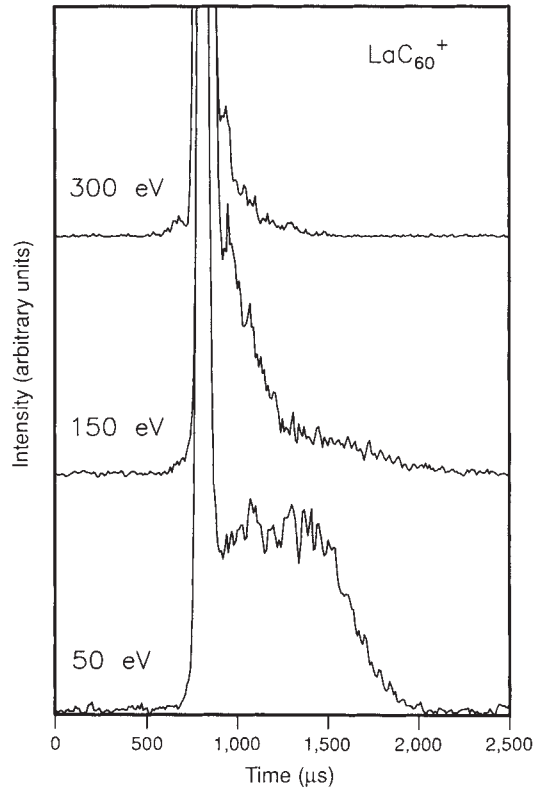

FIG. 2 Drift-time distributions recorded for LaC_{60}^+ as a function of injection energy (300, 150 and 50 eV). The experimental conditions were identical to those in Fig. 1.

To anneal the clusters, the injection energy is increased so that the ions experience a rapid transient heating cycle as their kinetic energy is thermalized by collisions with the buffer gas. The ions are then rapidly cooled by further collisions with the buffer gas. Any fragmentation that occurs is monitored using a second quadrupole mass spectrometer after the drift tube. Figure 2 shows drift-time distributions recorded for LaC_{60}^+ as a function of injection energy. As the energy is increased to 150 eV the relative abundance of isomers with drift times >1,300 μs (the roughly planar polycyclic ring isomers) rapidly diminishes, and at the same time there is an increase in the relative abundance of non-fullerene isomers with shorter drift times. As the injection energy is raised further, the relative abundance of the non-fullerene isomers with shorter drift times decreases. The polycyclic polyyne rings for LaC_{60}^+ anneal at lower injection energies than analogous C_{60}^+ isomers, indicating that the activation energy for annealing is lower for LaC_{60}^+ than for C_{60}^+.

Not all the LaC_{60}^+ isomers anneal into an intact metallofullerene. At high injection energies (300–400 eV), up to ~10% of the non-fullerene isomers fragment to products which appear to result from sequential loss of C_2 units. Figure 3 shows the drift-time distribution recorded for LaC_{58}^+ resulting from injection of LaC_{60}^+ at 200 eV. These results demonstrate that the fragment ions are entirely metallofullerenes. A careful search was performed for other fragment ions. The only other dissociation product observed was La^+ with a relative abundance of <1%. Thus it appears that nearly all the non-fullerene LaC_{60}^+ isomers anneal into metallofullerenes.

Figure 4 shows the drift-time distribution measured for

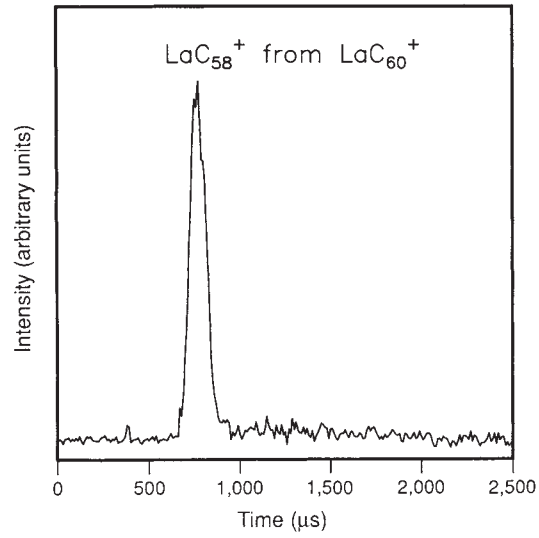

FIG. 3 Drift-time distribution recorded for LaC_{58}^+ resulting from LaC_{60}^+ injected into the drift tube at 200 eV. The experimental conditions were identical to those in Fig. 1. The only other product observed (except for the C_2 loss channels) was La^+. La^+ is substantially lighter than LaC_{60}^+, so there is a concern that the La^+ product could be discriminated against. Although there is no evidence for discrimination against the lighter products in previous studies[8], experiments were performed as a function of buffer gas pressure to be sure that any La^+ formed before the entrance to the drift tube was not scattered away by collisions with the buffer gas. In all cases, the relative abundance of La^+ was <1%.

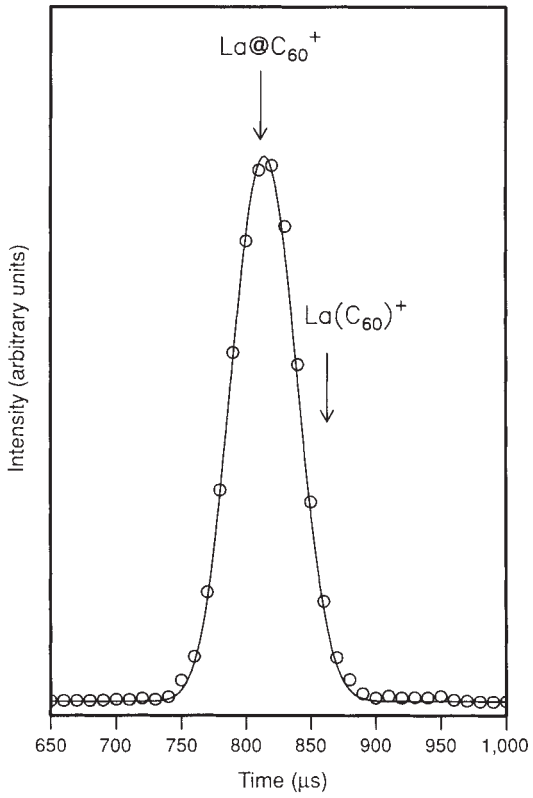

FIG. 4 Drift-time distribution (circles) recorded for LaC_{60}^+ with an injection energy of 400 eV. The solid line shows the drift-time distribution calculated from the transport equation for ions in the drift tube (see text). The arrows show the expected drift times for an endohedral $La@C_{60}^+$ and exohedral $La(C_{60})^+$ complex. The geometry of the exohedral $La(C_{60})^+$ was assumed to be a La atom sitting 2.4 Å from an unperturbed C_{60}. The mobility was calculated using a simple hard-sphere collision model[10] (details are given elsewhere[11]).

LaC_{60}^+ with an injection energy of 400 eV. At this high injection energy, all the non-fullerene isomers have annealed (or dissociated). The solid line in Fig. 4 shows the drift-time distribution calculated from the transport equation for ions in the drift tube[10]. The excellent agreement with the experimental results suggests that only a single LaC_{60}^+ isomer remains. Because the geometries of $La^+@C_{60}$ and $La(C_{60})^+$ are known, accurate drift times can be calculated from momentum transfer theory[10]. Arrows show the expected drift times[11] for an endohedral metallofullerene (which is assumed to be the same as for fullerene C_{60}^+) and an exohedral complex (where the lanthanum atom sits outside the fullerene cage). The measured drift time is in excellent agreement with that expected for the endohedral metallofullerene. The fragment ions (such as LaC_{58}^+) also appear to be endohedral metallofullerenes. A third isomer, where the lanthanum atom is incorporated into the fullerene cage, is also possible. Although the goemetry of this isomer is not well established, we estimate that the drift time for this species falls roughly half way between the arrows shown in Fig. 4. Our data show no signs of this isomer.

The remarkably high efficiency with which the non-fullerene LaC_{60}^+ isomers anneal into endohedral metallofullerenes indicates that there must be a mechanism by which the lanthanum atom is trapped inside the annealing fullerene. The distribution of non-fullerene LaC_{60}^+ ions shifts to shorter times as the clusters are annealed, indicating that in the first steps of the annealing process the LaC_{60}^+ complexes become more compact. The opposite behaviour is observed in the annealing of pure C_{60}^+, where the distribution of polyyne rings shifts to longer times as the polycyclic rings open to form bicyclic and monocyclic rings before forming the fullerene[6]. Because the ionization energy of La (5.577 eV)[12] is substantially lower than that of fullerene C_{60} (7.62 eV)[13], the charge is probably localized on the lanthanum. Therefore, a plausible explanation for the behaviour of the non-fullerene LaC_{60}^+ isomers is that the La^+ acts as a nucleation centre, and the carbon rings arrange themselves around the La^+ so that when they anneal into the fullerene cage the lanthanum atom is naturally encapsulated. Electrostatic interactions may play an important role in arranging the carbon rings in the early stages of the annealing process. This simple picture of the annealing mechanism accounts for both the shift to shorter times and the high efficiency of endohedral metallofullerene formation. □

Received 15 November; accepted 22 December 1993.

1. Heath, J. R. *et al. J. Am. chem. Soc.* **107,** 7779–7780 (1985).
2. Bethune, D. S., Johnson, R. D., Salem, J. R., deVries, M. S. & Yannoni, C. S. *Nature* **366,** 123–128 (1993).
3. Chai, Y. *et al. J. phys. Chem.* **96,** 7564–7568 (1991).
4. McElvaney, S. W. *J. phys. Chem.* **96,** 4935–4937 (1992).
5. McElvaney, S. W., Ross, M. M., Goroff, N. S. & Diederich, R. *Science* **259,** 1594–1596 (1993).
6. Hunter, J. M., Fye, J. & Jarrold, M. F. *Science* **260,** 784–786 (1993).
7. von Helden, G., Gotts, N. & Bowers, M. T. *Nature* **363,** 60–63 (1993).
8. Hunter, J. M., Fye, J. L., Roskamp, E. J. & Jarrold, M. F. *J. phys. Chem.* (in the press).
9. von Helden, G., Hsu, M.-T., Kemper, P. R. & Bowers, M. T. *J. chem. Phys.* **95,** 3835–3837 (1991).
10. Mason, E. A. & McDaniel, E. W. *Transport Properties of Ions in Gases* (Wiley, New York, 1988).
11. Jarrold, M. F. & Bower, J. E. *J. chem. Phys.* **98,** 2399–2407 (1993).
12. Rosenstock, H. M., Draxl, K., Steiner, B. W. & Herron, J. T. *J. phys. Chem. Ref. Data (Suppl. No. 1)* **6,** (1977).
13. Zimmerman, J. A., Eyler, J. R., Bach, S. B. & McElvany, S. W. *J. chem. Phys.* **94,** 3556–3562 (1991).

ACKNOWLEDGEMENTS. We thank P. Halasyamani and K. Greenwood for assistance with preparing the La_2O_3/graphite rod, and J. Hunter and J. Fye for discussion. This work was supported in the US by the NSF.

Quantitative self-assembly of a [2]catenane from two preformed molecular rings

Makoto Fujita, Fumiaki Ibukuro, Hideaki Hagihara & Katsuyuki Ogura

Department of Applied Chemistry, Faculty of Engineering, Chiba University, 1-33 Yayoicho, Inageku, Chiba 263, Japan

MOLECULES composed of interlocking rings are termed catenanes. Since the first synthesis of a two-ring catenane (a [2]catenane) in 1960[1], these and related interlinked compounds have attracted considerable interest[2–10], in part from the perspective of forming molecular devices and nanoscale architectures[11,12]. Here we report the formation of a [2]catenane from two complete rings, reminiscent of the trick of interlinking 'magic rings'. This supermolecule, 1 in Fig. 1, exists in rapid equilibrium with the monomeric rings 2, as revealed by ^{1}H NMR and electrospray mass spectrometry. At low concentration of molecule 2, the equilibrium lies towards the monomers, but at higher concentrations the catenane is the overwhelmingly dominant species in solution.

Previous syntheses of catenanes have all taken the approach of threading a ring on a thread and then linking the ends of the thread. In the syntheses of Stoddart and coworkers[3–6], for example, the ring and thread self-assemble so that the ends of the thread lie adjacent to one another and can readily be capped by a bridging unit. Our present approach exploits the relatively labile nature of metal–ligand bonds, which comprise a part of the rings, to interlock two preformed rings in solution.

When a D_2O solution of the Pd(II) complex (en)$Pd(NO_3)_2$ (en, ethylenediamine) (**3**) (1 mM) was treated with the 1.0 molar equivalent 1,4-bis[(4-pyridyl)methyl]benzene (**4**), ^{1}H NMR